Computer Physics Communications 185 (2014) 1628–1638

Contents lists available at ScienceDirect

Computer Physics Communications

journal homepage: www.elsevier.com/locate/cpc

Arbitrary perturbations in Monte Carlo neutral-particle transport

James Tickner *

CSIRO Centre for Process Science and Engineering, Building 67, Lucas Heights Science and Technology Centre, New Illawarra Road, Lucas Heights, NSW 2234, Australia

ARTICLE INFO

Article history:
Received 21 March 2013
Received in revised form
27 February 2014
Accepted 1 March 2014
Available online 11 March 2014

Keywords:
Monte Carlo
Perturbation methods
Neutral-particle transport
EGS

ABSTRACT

Monte Carlo techniques are widely used to model particle transport in complex models, as both the transport physics and level of geometric details can be simulated with arbitrary precision. The major draw-back of the Monte Carlo method is its computational cost. This is particularly true in design studies, where the effects of small changes in the model may be masked by statistical fluctuations unless prohibitively long simulation times are used. Perturbation methods have been developed to model the effects of small changes in material density, composition or reaction cross-sections. In this paper, I describe how this approach can be extended to allow nearly arbitrary perturbations in the transport problem specification to be made, including material properties, the model geometry and the radiation source description. The major problem, handling arbitrary variations in the model geometry, is overcome using a modified form of the Woodcock neutral-particle tracking algorithm. The approach has been implemented as an extension to the general-purpose Monte Carlo code EGSnrc. I discuss the details of this implementation, including how the specification of a perturbation simulation can be generated automatically from two or more unperturbed simulation models. I present an example of the application of the method to the modelling of a simple X-ray fluorescence instrument.

1. Introduction

Monte Carlo methods can be used to solve the radiation transport problem by performing a direct, microscopic simulation of individual radiation quanta. The energy, direction and other properties of a particle emitted by a radiation source are sampled from the appropriate distributions. The location and nature of the particle's interactions with the materials comprising the underlying system geometry are similarly sampled, the energy, type and nature of the particles arising from the interaction are determined, and the process repeated until the particle is captured, escapes or is otherwise terminated. Contributions to quantities of interest (*tallies*), such as flux or energy deposition, are recorded during the transport process. By simulating a large number of source particles N, average tally results can be estimated with a statistical precision that improves like $N^{-1/2}$.

The relatively slow convergence of the Monte Carlo method is a particular problem when estimating the effects produced by small variations in the problem specification. If two separate simulations are performed of slightly different problems, then in general the particle transport in the two runs quickly diverges, meaning that the statistical errors on the two simulations are uncorrelated. Very large number of events may then have to be simulated to estimate the effect of the variation with any confidence.

A partial solution to this problem is correlated-history sampling. Normally, the random sampling of source particle properties and subsequent interactions is carried out by drawing numbers sequentially from a pseudo-random number generator. Even if identical generators are used in separate simulations, as soon as one particle takes a different path (usually requiring a different number of random numbers to track its subsequent collisions), the pseudo-random number sequences used in the two simulations become desynchronised. From this point on, the events simulated in the two simulations are completely uncorrelated. The correlated-history approach insists that each simulated event starts at a known place in the random number sequence. A large number of random samples are allocated to each event, of which only a fraction are normally required. Unused samples are discarded at the end of each event and the random number generator is reset to the correct starting point for the next event to be simulated. For example, the MCNP code [1] allocates 152,917 random samples per event and uses a linear congruential generator that allows efficient skipping over the samples that are not required.

* Tel.: +61 8 8303 8430; fax: +61 2 9710 6732.
E-mail address: james.tickner@csiro.au.

http://dx.doi.org/10.1016/j.cpc.2014.03.003
0010-4655/

The correlated-history sampling approach improves the correlation between the errors on the separate runs, reducing the error on the difference in the tally quantity of interest. However, for individual events where the variation in the problem specification causes particles to follow different paths, particle transport in the two runs is uncorrelated as soon as the divergence occurs, so the correlation is not perfect. Further, by requiring two separate runs to be performed, the approach doubles the required simulation time.

For changes in material composition or density, or to estimate uncertainties due to using different cross-section evaluations, the perturbation approach is well known [1–8]. A single set of particle histories is generated and used to calculate tally quantities for both the original problem and for one or more variations, termed *perturbations*. This leads to very strong correlation in the statistical errors for the original and perturbed problems, and consequently small errors on the difference in tally results. For each perturbation, a perturbed weight parameter is introduced. Starting at unity, the value of this parameter is altered whenever a particle is transported or undergoes an interaction, by multiplying it by the ratio of the probability of the transport or interaction process occurring in the perturbed problem to the probability of it occurring in the original problem. Whenever a tally is made, the tally quantity for the perturbed problem is equal to the tally for the unperturbed problem multiplied by the perturbed weight.

The perturbed weight multiplying factors arising during particle transport can be estimated by Taylor expansion [5], also known as the differential approach, or by the multiple-estimation method [6], also known as correlated sampling. For the rest of this paper, I use the correlated sampling approach, as the perturbation estimates are correct to all orders and the calculations are considerably simpler, particularly compared to the evaluation of second or higher order terms in the Taylor expansion approach. The main advantage of the differential technique is held to be that as derivatives are explicitly calculated, one can perform *a posteriori* sensitivity calculations [8]. I argue however, that the effects of multiple perturbations can be calculated in a single run at low computational cost using the correlated sampling approach and *a posteriori* results for perturbations of intermediate magnitude estimated using interpolation.

In comparison to the problem of perturbations to materials and cross-sections, methods for handling variations in problem geometry have received much less attention. Takahashi [9] describes a scheme that allows the effects of simple geometric variations to be estimated. Shuttleworth [10] discusses the application of this technique in the MCBEND Monte Carlo code. Sitaraman [11] introduces a method for calculating sensitivity to surface changes using first-order perturbation theory, and describes the incorporation of this method into a customised version of the MCNP code.

In this paper, I discuss how the perturbation approach can be extended to allow nearly arbitrary variations to be made to the materials, geometry and radiation sources in a simulation. The motivation for this work is to further the use of the Monte Carlo method for designing and optimising X-ray and neutron-based analysis instruments. The availability of what is essentially derivative information (a Hessian matrix) – in other words, changes in tally quantities with respect to parameterised changes in instrument design – serves two purposes. Firstly, it provides some direction on how a design might be modified to improve instrument accuracy, for example by making changes that reduce the statistical error of an analysis. Secondly, it provides information about the size of instrumental systematic, or non-statistical errors, arising, for example, due to an inaccurately positioned sample, or variation in the output of the radiation source.

The remainder of this paper is structured as follows.

Section 2 revisits the material perturbation technique and demonstrated how, in combination with the Woodcock tracking algorithm, it can be extended to calculate the effects of changing the size, shape or position of geometric regions. The more straightforward extension of the material perturbation technique to variations in the energy or angular distributions of particles emitted by the source is also described.

Section 3 discusses the handling of common types of Monte Carlo tallies in perturbation problems.

Section 4 describes the process by which the rather complex specification of simulations including one or more perturbations can be produced automatically from the descriptions of the original problem and its variations. An important consideration is what I term the 'super-set' problem, namely ensuring that all process that can occur at any point in any of the perturbed variations have non-zero probability of occurring at that point in the primary simulation.

Section 5 presents results for an example problem, namely a simple model of an X-ray fluorescence analyser incorporating an X-ray tube and silicon detector. The perturbation approach is used to estimate the errors resulting from movement of the sample or detector, a change in sample density and composition and a fluctuation in the operating voltage of the X-ray tube. Some comments on the efficiency of the perturbation approach are also presented.

Section 6 outlines the conclusions arising from this work.

2. The perturbation method

There is a close correspondence between the perturbation method and approaches for statistical variance reduction in Monte Carlo transport. Both rely on the introduction of a numerical factor termed 'weight' to allow particle properties to be sampled from non-physical or so-called non-analogue distributions.

Suppose that the properties $\mathbf{x}$ (for example, energy and direction) for a particle produced by a radiation source or in collision should be sampled from a physical distribution $p(\mathbf{x})$. We can sample the properties from an alternative distribution $q(\mathbf{x})$ provided that we multiply the particle's current weight by a factor

$$r = p(\mathbf{x})/q(\mathbf{x}). \tag{1}$$

Particle weights start at unity and may increase or decrease as the transport of the particle proceeds. Whenever a particle makes a tally contribution, that contribution must be multiplied by a statistical weight factor. For a simple, Boltzmann tally which does not depend on inter-particle coincidences, the statistical weight factor is given simply by the particle weight. For non-Boltzmann tallies where coincidences are important, the calculation of the statistical weight factor is more complicated. This is discussed in more detail in Section 4.

When playing variance reduction games, the user attempts to find non-physical distributions that result in a reduction in the statistical error achievable in a given amount of computer time. For example, these games may involve randomly terminating particles that are deemed unlikely to make a tally contribution, whilst increasing the weight of any survivors to ensure the process is unbiased.

The correspondence with the perturbation method is straightforward. Suppose that we sample all particle properties from the distributions corresponding to the normal, unperturbed problem. Tally outputs are recorded with a unit weight factor, and the tally results correspond to those expected for the unperturbed problem. In parallel however, we can calculate a perturbed weight factor, given by

$$r_p = p'(\mathbf{x})/p(\mathbf{x}) \tag{2}$$

where $p'(\mathbf{x})$ and $p(\mathbf{x})$ are the probabilities of a given interaction occurring in the perturbed and unperturbed problems respectively.

A tally recorded with a statistical weight factor equal to the perturbed weight will then record the tally contribution expected for the perturbed case. The perturbed and unperturbed tally contributions can be recorded in parallel from the same set of sample histories, resulting in maximally correlated statistical errors for the two cases and minimal computational overhead.

Variance reduction and perturbation techniques can be combined in a single simulation. Particle properties are sampled from arbitrary distributions, chosen to minimise variance. Separate weight factors are calculated for the unperturbed problem, using Eq. (1), and for the perturbed variations, using Eq. (2). Tallies for the unperturbed problem use a statistical weight factor equal to the unperturbed particle weight, and tallies for the perturbed variations use a statistical weight factor equal to the product of the unperturbed and perturbed particle weights.

The following sections describe the calculation of the perturbed weight factors for variations in material, geometry and source specification.

Material perturbations

In this subsection, I consider the case where the geometry model of the problem is the same in perturbed and unperturbed cases, but the density and/or composition of materials filling one or more regions of the model differ. The treatment closely follows the approach originally outlined by Rief [5].

Consider one step in a particle's history, comprising one transport step and one collision. The particle starts with properties $\mathbf{x_i}$ and finishes with properties $\mathbf{x_{i+1}}$. For definiteness, let us take the essential particle properties to be a position (x, y, z), direction cosine vector (u, v, w) and energy E. The particle starts with energy E_i at position (x_i, y_i, z_i) and travels a distance d_i in direction (u_i, v_i, w_i) to position $(x_{i+1}, y_{i+1}, z_{i+1})$. At this position, it makes a collision which changes both its direction and energy.

The perturbed weight factor for this step is given by the product of two factors:

$$r_p(i) = T_i R_i \tag{3}$$

where T_i and R_i are factors associated respectively with the transport of the particle between collision points and the probability of a particular reaction occurring at the point $(x_{i+1}, y_{i+1}, z_{i+1})$.

The factor T_i is the ratio of the probabilities of a particle travelling a distance d_i without making a collision in the perturbed and unperturbed cases, given straightforwardly by

$$T_i = \frac{\exp(-\Sigma_p)}{\exp(-\Sigma)} = \exp(\Sigma - \Sigma_p) \tag{4}$$

where Σ is the number of interaction lengths (mean-free paths) for particles of energy E between points (x_i, y_i, z_i) and $(x_{i+1}, y_{i+1}, z_{i+1})$ in the unperturbed problem, given by the integral of the macroscopic cross-section along the straight-line path connecting these points. The quantity Σ_p is the same parameter evaluated for the perturbed problem.

In practice, Monte Carlo geometry models normally comprise a finite number of homogeneous regions bounded by simple surfaces—planes, quadrics and tori. In regions that contain the same material in both perturbed and unperturbed problems, Eq. (4) reduces to unity. Eq. (4) can then be written as

$$T_i = \exp\left(\sum_j \left(\mu_p^j - \mu^j\right) d_{ij}\right) \tag{5}$$

where μ^j is the macroscopic cross-section in the jth region in the unperturbed problem, μ_p^j the cross-section in the same region in the perturbed problem, d_{ij} is the length of the portion of the particle track segment i that lies in region j and the sum extends over all regions intersected by the particle's track segment that contain different materials in the perturbed and unperturbed problems.

The factor R_i is the ratio of the probabilities of a particular reaction k occurring in an infinitesimal distance Δd at the point $(x_{i+1}, y_{i+1}, z_{i+1})$ in the perturbed and unperturbed cases, given by

$$R_i = \frac{\sigma_k N_p \Delta d}{\sigma_k N \Delta d} = \frac{N_p}{N} \tag{6}$$

where σ_k is the microscopic cross-section for reaction k, and N_p and N are the number densities of the atomic species (or isotopic species for neutron transport simulations) responsible for the reaction in the perturbed and unperturbed problems.

Combining Eqs. (3), (4) and (6), the perturbed weight factor is then given by the simple result

$$r_p(i) = \exp(\Sigma - \Sigma_p)\,\frac{N_p}{N}. \tag{7}$$

Both factors appearing in Eq. (7) can be readily calculated, once the regions through which the particle track segment pass are known and the reaction occurring at the collision point has been sampled. These calculations need to be made during normal particle transport, so the additional calculations for the determination of the perturbed result can be made with minimal computational overhead.

Geometry perturbations

Perturbations to the model geometry can be formally handled in exactly the same way as perturbations to material densities or compositions. For any given transport step i, the perturbed weight factor can be written as a product of two probability ratios: the first being the ratio of probabilities in the perturbed and unperturbed problems of the particle reaching the collision point $i + 1$, and the second the ratio of the probabilities of the particle undergoing a particular reaction k at this point. Eq. (7) can then be used to calculate the perturbed weight factor for transport step i.

The main difficulty lies in the efficient calculation of the factors appearing in Eq. (7) for the general case, particularly the transport factor T_i.

Takahashi [9] describes an effective solution for the simplest cases (Fig. 1). He considers the effect on the reactivity of a pulsed fast-neutron reactor induced by a small displacement of a reflector block. The block, which has the form of a rectangular prism, is displaced along its length. The effect of the displacement is to generate 3 regions: one which (I) is initially filled, but voided in the perturbed problem; a central region (II) which is filled in both problems, and a final region (III) which is initially empty, but filled in the perturbed problem. The geometry perturbation problem then reduces to an instance of a material perturbation problem, with the regions at either end of the block alternately filled or voided in the perturbed and unperturbed cases.

There are two problems with extending this approach to more general geometric perturbations.

The first arises from the 'unvoiding' of region III—that is, changing its composition from empty (vacuum) in the unperturbed problem to filled in the perturbed case. By definition, no collisions can occur in this region in the unperturbed problem, so there is no sampling of the collisions that should occur in this region in the perturbed case. Takahashi describes a solution, based on an analytical estimate of the interaction probability of neutrons entering this region. However, it is not clear how this approach could be easily extended to more complex geometry cases. This is a specific instance of the more general 'super-set' problem that I will return to in Section 3.

The second problem is a combinatory one. Consider a problem with N separate regions, each of which may be subject to a

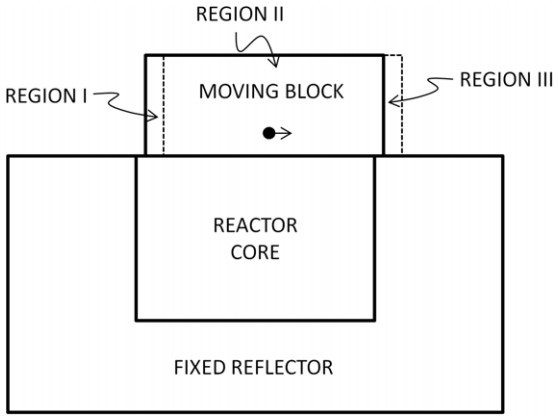

Fig. 1. Illustration of elementary geometric perturbation (adapted from Takahashi [9]).

perturbation of shape, size or position. In general, N^2 overlapping regions may be produced. If we wish to simulate M separate perturbations in a single run, then N^{M+1} overlap regions may result in the worst case. Whilst real problems will rarely reach this level of complexity, determining region overlaps and specifying a single geometry model that covers all of the perturbations rapidly becomes impossible. Tracking particles through such a complex geometry model will also reduce performance.

A second approach would be to directly calculate the factor T_i for each of the M perturbations. Separate geometry models for the unperturbed and M perturbed cases would be stored in computer memory. The locations of the collision points would be sampled with reference to the unperturbed geometry model and the value of Σ calculated. For each of the M perturbed cases, the number of interaction lengths Σ_P would be evaluated, allowing T_i to be directly calculated.

This approach, whilst straightforward to implement, would lead to an unacceptable degradation in performance. The calculation of the number of interaction lengths between two points involves breaking the track segment into pieces each time it crosses from one region to the next. The calculation of these break points is particularly expensive, involving the determination of the intersection of the particle's direction with each surface of the current region, the sorting of these interaction distances into ascending order and finally the systematic determination of whether the intersection points lie inside or outside the region.

Profiling of an X-ray transport simulation based on the EGSnrc [12] Monte Carlo package shows that 76% of the processing time (excluding time for program initialisation and termination) is taken up by the geometry interrogation routines. Only 21% of the processing time is associated with the 'physics' subroutines—cross-section interpolation, reaction sampling and determination of the properties of reaction products. The remaining time is used for tallying and other book-keeping functions. A naive implementation of the calculation of T_i could be expected to lead to a near-linear decrease in performance with the number of perturbations modelled.

These difficulties can be avoided by using a modified version of the Woodcock [13] or delta-tracking algorithm. The Woodcock algorithm provides a method for sampling the position of the next interaction of a neutral particle in a Monte Carlo transport simulation without the calculation of distances to region boundaries. With modifications that I describe below, it can be used to calculate values for T_i without explicit segmentation of particle track segments across regions.

Consider a particle that has just been emitted from the source or emerged from a collision. The problem is to sample where the next interaction of this particle occurs, given the direction of the particle.

The normal approach is to sample the number of interaction lengths λ to the next collision from the exponential distribution $\exp(-\lambda)$. The distance to the first boundary of the region containing the particle, d, is calculated. If the value of λ is less than $d\mu$, where μ is the macroscopic cross-section of the material, then the interaction occurs inside the current region at a distance λ/μ from the previous collision, otherwise the particle is moved to the boundary of the current region and the process repeated.

The Woodcock algorithm works by adding a fictitious interaction – the delta-interaction, that leaves all properties of the particle unchanged – to the normal reaction processes. The cross-section for the delta-interaction for each material is chosen so that all materials in the problem have the same total cross-section. If all materials have the same total cross-section, then the distance travelled to the next collision is given simply by λ/μ, with λ sampled from an exponential distribution and μ equal to the total cross-section, including the fictitious delta-interaction. To sample the reaction that occurs at the collision point, the region containing this point must be determined. When sampling the nature of the collision that occurs, the delta-interaction must be included in the list with the normal, physical reaction processes with the appropriate probability. If sampling results in the occurrence of a delta-interaction, then the particle properties are left unchanged.

The Woodcock algorithm eliminates the need for calculating distances to boundary crossings, at the cost of requiring more calls to the subroutine that identifies in which region a given point lies. However, the computational cost of the region-determination function is generally much less than that of the boundary-distance function.

Calculating perturbed weight factors using the Woodcock approach is straightforward.

Firstly, the transport factor T_i is trivially equal to unity in all cases, as all materials have the same total cross-section, once the delta-interaction is included.

As before, the reaction factor R_i is given by the ratio of the probabilities of the given reaction occurring the perturbed and unperturbed cases. If a delta-interaction was sampled for the unperturbed case, then R_i is given by

$$R_i = \frac{\delta_p}{\delta} \tag{8}$$

where δ and δ_p are the ratios of the delta-interaction cross-section to the total material cross-section for the material present at the collision point in the unperturbed and perturbed cases respectively.

If a normal, physical reaction was sampled, then R_i is given by

$$R_i = \frac{(1-\delta_p)}{(1-\delta)}\frac{N_p}{N} \tag{9}$$

where, as before, N and N_p are the atomic (or isotopic) number density for the species involved in the reaction in the unperturbed and perturbed cases respectively.

With T_i equal to unity, the perturbed weight factor for transport step i, $r_p(i)$, is given simply by $r_p(i) = R_i$, with R_i evaluated using Eq. (8) if a delta-interaction occurs and Eq. (9) if a normal, physical reaction is sampled.

A comment should be made about the selection of the magnitude of the delta-interaction cross-section. Normally, the cross-section is chosen to be zero for the material with the largest physical cross-section at the current particle energy. This minimises the total cross-section, ensuring that the average distance between sampled interaction points (equal to $1/\mu$) is as large as possible and thereby improving the efficiency of the tracking process.

This approach introduces a problem, however. Consider an example where a region containing the material with the largest cross-section in the unperturbed case is modified to contain a material with a lower cross-section in the perturbed problem. Clearly, there is a non-zero probability of delta-interactions occurring in the perturbed case, as the delta-interaction cross-section is also non-zero. However, if the delta-interaction cross-section for the material in the unperturbed problem is zero, then these interactions will never be sampled. This is another instance of the 'super-set' problem that is discussed in Section 3.

The solution to this problem is straightforward: the delta-interaction cross-section must be non-zero for all materials. A value of $\delta = 0.2$ for the material with the largest cross-section is found to work well; δ-values for materials with smaller cross-sections are correspondingly larger. A minimum δ value of 0.2 increases the number of calls to the region-determination function by 20% compared to the optimal case, but limits large fluctuations in the perturbed weight factor; in the worst-case, where a region containing the material with the largest cross-section in the unperturbed problem is converted to vacuum in the perturbed case, $R_i = 5$.

Source perturbations

The last type of perturbation that I consider is variations to the emission rate, energy spectrum and angular distribution of particles produced by the radiation source. Suppose that the source in the unperturbed problem emits I particles per second with a normalised probability distribution $S(\mathbf{x})$, where $\mathbf{x}$ represents a vector of relevant phase space variables for the emitted particle: position, energy, direction, time etc. Let the equivalent parameters for the perturbed case be I_p and $S_p(\mathbf{x})$.

The starting parameters of the source particle in the unperturbed problem may be sampled in an analogue fashion from S (in which case the particle is started with unit weight), or they be sampled from a biased distribution and the source particle started with a compensatory non-unit weight.

In either case, the initial perturbed weight factor, $r_p(0)$, is given simply by the ratio of the number of particles that would be produced with these phase–space parameters in the perturbed and unperturbed cases:

$$r_p(0) = \frac{I_p}{I}\frac{S_p(\mathbf{x})}{S(\mathbf{x})}. \tag{10}$$

A case of particular interest is when the radiation source is an X-ray tube. An X-ray tube produces X-rays by accelerating electrons through a fixed potential onto a metal target, producing both continuum Bremsstrahlung radiation and characteristic fluorescence lines from the target element. Small variations in the accelerating potential change both the overall intensity, the shape of the Bremsstrahlung continuum and the intensities of the characteristic lines.

The X-ray energy spectrum is to a good approximation independent of the emission angle, meaning that Eq. (10) reduces to

$$r_p(0) = \frac{I_p}{I}\frac{S_p(E)}{S(E)} \tag{11}$$

where E is the X-ray energy. Various semi-analytical expressions for I and $S(E)$ are available in the literature [14–16].

3. Treatment of tallies

Modern Monte Carlo codes use a wide variety of different tallies to efficiently estimate parameters of interest from the simulated particle histories. In this section, I consider three broad classes of tally: collision- and track-based estimators, next-event estimators and non-Boltzmann or coincidence tallies. I also describe how uncertainties in the estimated tally results can be calculated for both perturbed and unperturbed cases.

Collision- and track-based estimators

The simplest case occurs when the tally contribution arises in a region where no perturbation applies—that is, the geometry of that region and the material that it contains are the same in the perturbed and unperturbed problems. In this case, the magnitude of the tally contribution is the same in all problems, and only the weight with which this contribution is made differs.

Suppose that a tally contribution of magnitude t is made by a particle with weight (in the unperturbed problem) of w. The weight of the particle in the perturbed problem, w_p is given by

$$w_p = w\prod_{i=0}^{n} r_p(i) \tag{12}$$

where the product extends over the n collisions made by the particle before the tally contribution occurs. The recorded tally contributions in the unperturbed and perturbed cases are then given by wt and $w_p t$ respectively.

If the region where the tally occurs *is* subject to a perturbation, then the magnitude of the tally contribution will be different in the perturbed and unperturbed cases, and the tally contribution recorded for the perturbed case is then given by $w_p t_p$ where t_p is the magnitude of the perturbed tally contribution.

Collision-based estimators are by definition associated with a collision at a single point. Consequently, the only information that needs to be determined is the region containing that point and the material filling that region in the unperturbed and perturbed cases. In practice, this information will have been determined as part of the calculation of reaction factor R for the collision.

If the quantity being tallied depends on the total cross-section only (including the delta component), then the magnitude of the tally contribution is the same in the perturbed and unperturbed cases, unless a geometry perturbation causes the collision point to lie in different regions in the perturbed and unperturbed problems.

For example, consider the case of estimating the particle flux in a given region j using a collision-based estimator. Suppose that the collision occurs in region i in the unperturbed case and in region i_p in the perturbed case. The volumes of the regions in the two cases are V_i and V_{i_p} respectively. The total macroscopic cross-section, including the delta-interaction component, is the same in the two cases and given by μ. The flux contribution in the unperturbed case can then be written as

$$t_{\text{flux}} = \frac{\delta_{ij}}{\mu V_i} \tag{13}$$

where δ is the Kronecker delta function.

The flux contribution in the perturbed case is given by

$$t^p_{\text{flux}} = \frac{\delta_{i_p j}}{\mu V_{i_p}}. \tag{14}$$

Track-based estimators include surface-crossing tallies (measuring, for example, the current of particles across a surface, or the average flux on the surface of a region) and track-length estimators for particle flux. As track-estimators are, by definition, based on the properties of a track segment, they depend on the properties of the region(s) that contain that segment.

For example, reconsider the case of estimating the particle flux in a region j, this time using a track-length based flux estimator.

The flux contribution for unperturbed case is given by

$$t_{\text{flux}} = \frac{d_j}{V_j} \tag{15}$$

where d_j is the length of the portion of the current track segment that lies inside region j. This length may be zero if the track segment does not intersect this region. Similarly, the flux contribution for the perturbed case is given by

$$t^p_{\text{flux}} = \frac{d^p_j}{V_j} \tag{16}$$

where d^p_j is the length of the portion of the current track segment that lies inside region j in the perturbed case.

As noted previously, explicit evaluation the lengths of the track segments lying inside region j is relatively expensive, and the calculation must be repeated for each perturbed problem variation if it is determined that the particle track segment lies in a region containing perturbations. However, with careful specification of the problem geometry, this calculation only needs to be carried out for the limited fraction of track segments that are highly likely to record a tally score, as described in the following section.

Next-event estimators

Next-event estimators refer to a broad class of tallies that estimate particle flux, or derived quantities such as flux or interaction rate at a point remote from the current particle track. They provide a powerful variance reduction tool for problems where it is desired to tally particles in a geometrically small region that is unlikely to be sampled in normal particle transport. Next-event estimators are so-named because at each collision, they analytically estimate the probability of the scattered particle reaching a particular point or region without further interaction.

The canonical next-event estimator is the point-flux tally [17]. Suppose that a particle has just undergone a collision and a reaction product with energy E has been sampled. The flux contribution at a particular point P from this collision is given by:

$$\Omega t_{\text{flux}} = \frac{\exp(-\Sigma)}{D^2} \cdot \frac{1}{\sigma}\frac{\delta\sigma}{d} \tag{17}$$

where Σ is the number of interaction lengths (mean-free paths) between the collision point and P for a particle of energy E, D is the distance from the collision point to P and $\Omega\frac{1}{\sigma}\frac{\delta\sigma}{d}$ is the normalised differential cross-section for the incident particle to be scattered towards P.

As the cross-section term in Eq. (17) is normalised, the same result applies whether or not the region where the collision occurs is subject to a perturbation. Any variation in material composition at the collision point (due to either a material or geometry perturbation) is accounted for by the collision factor R (Eqs. (6), (8) and (9)). However, the material attenuation factor $\exp(-\Sigma)$ should be replaced by $\exp(-\Sigma_p)$ in the perturbed problem case.

Just as for the track-length case, the evaluation of Σ in the unperturbed and perturbed cases is expensive. However, a simple variance reduction scheme can be employed to minimise this cost. Users assign to each region a probability p with which the next-event estimation should be carried out for particles making collisions in that region. If a number chosen from a random, uniform distribution covering the range [0, 1] is less than p, then the next-event flux contribution is made, weighted by an additional factor of $1/p$, otherwise no estimate is made. Regions from which contributions are expected to be small are assigned a low value of p, minimising the number of computationally expensive evaluations made for scattering events in these locations.

Coincidence tallies

Coincidence, or non-Boltzmann tallies are those that depend on the properties of two of more tracks or collisions. The most commonly encountered example is the energy deposition tally, which records the physical deposition of energy in a region such as a detector. Typically, a particle may make several interactions in the region, and the energy lost in each collision is summed to determine the total energy deposition. For example, a high-energy gamma-ray may make several Compton (inelastic scattering) interactions before its energy falls far enough for it to be absorbed photoelectrically and its track terminated. In what follows, I shall restrict discussion to energy deposition tallies, although the approach can be readily extended to other non-Boltzmann tallies.

Compared to the simpler tally types discussed above, where the tally contributions can be recorded as the properties of individual collisions or track segments are sampled, coincidence tallies require more complicated record keeping and post-event processing in problems that include variance reduction or perturbations.

Suppose, for example, that a particle with weight w_1 deposits energy E_1 inside a particular region. After undergoing a variance reduction game, its weight is modified to w_2 and it deposits a further energy E_2 in the same region. What energy should be recorded into the tally, and with what magnitude should the contribution be scored?

In [18] I describe an algorithm for efficiently answering these questions for simulations that include variance reduction, which is based on the earlier work of Booth [19]. During particle transport, each energy deposition in a sensitive (or tally) region is noted in a table, along with the weight of the particle at the time the deposition occurs, and additional information that allows the event history to be reconstructed. Specifically, this additional information allows the energy deposition events to be grouped according to whether they are associated with physically related particles (for example, particles originating from a single collision), or whether they arise from variance reduction processes that generate additional particle tracks, or change particle weights.

A post-processing function that runs after each event reconstructs the event history and determines the tally entries that should be made, in terms of the magnitude of the energy deposition and the weight with which it should be recorded.

The extension of this algorithm to problems that include perturbations is straightforward. As the perturbed particles follow exactly the same paths and are subject to the same variance reduction processes at the unperturbed particles, both have exactly the same event history.

Importantly, in neutral-particle transport simulations, the energy deposition process can be considered as a 'point-like' interaction associated with a particular collision. That is, the physical deposition process, which is associated with the production and energy loss of a charged particle such as an electron or proton, normally occurs over a length-scale that is small compared with the distances travelled by the original neutral particles. This means that the only additional information required is the region containing the collision point in the perturbed case. In practice, the region will have already been identified as part of the calculation of the collision factor R.

Each time an energy deposition occurs, the following information is recorded: the deposited energy; the identity of the region containing the collision point and the particle weight in the unperturbed case; the identity of the region containing the collision point and the particle weight in the perturbed case; and additional

information to enable event history reconstruction (identical for the two cases).

During the reconstruction of the event history that occurs during post-processing, the total energy deposition in each sensitive region and the weight with which the tally contributions should be made can be simultaneously calculated for the unperturbed and perturbed cases using the information recorded in the event table.

Uncertainty estimation

All quantities estimated using the Monte Carlo method have an inherent statistical uncertainty. It is important that any code return an estimate of this uncertainty to allow the user to determine the significance of their results.

Suppose that N events are simulated and that the tally contribution in the unperturbed case for event i is t_i. For sufficiently large N, the relative uncertainty on the estimated average tally contribution $\bar{t} = \frac{1}{N}\sum_i t_i$ is given by

$$\frac{\sqrt{E\left[\bar{t} - E(\bar{t})\right]^2}}{\bar{t}} = \frac{1}{\bar{t}}\sqrt{\frac{\mathrm{var}(t)}{N}} = \frac{1}{\bar{t}}\sqrt{\frac{\sum(t_i - \bar{t})^2}{N^2}} = \sqrt{\frac{\sum t_i^2}{\left(\sum t_i\right)^2} - \frac{1}{N}} \tag{18}$$

where E denotes expectation value and $\mathrm{var}(t)$ denotes the variance of the distribution of tally contributions. The last transformation in Eq. (18) demonstrates that only two running sums (t and t^2) need to be retained during particle transport to calculate the final error.

For the perturbed case, the quantity of most interest is the relative error on the difference between the estimated tally values for the perturbed and unperturbed cases. Following Rief [7], the relative error can be written as

$$\frac{\sqrt{E\left[(\bar{t}_p - \bar{t}) - E\left(\bar{t}_p - \bar{t}\right)\right]^2}}{|\bar{t}_p - \bar{t}|} = \frac{1}{\bar{t}_p - \bar{t}}\sqrt{\frac{\mathrm{var}(t) + \mathrm{var}(t_p) - 2\mathrm{covar}(t, t_p)}{N}}$$

$$= \frac{1}{\bar{t}_p - \bar{t}}\sqrt{\sum t_i^2 + \sum t_{ip}^2 - 2\sum t_i t_{ip} - \left[\left(\sum t_i\right)^2 + \left(\sum t_{ip}\right)^2 - \sum t_i \sum t_{ip}\right]/N} \tag{19}$$

where $\mathrm{covar}(t, t_p)$ denotes the covariance between unperturbed and perturbed tally contributions. Evaluating Eq. (19) requires five running sums to be retained during particle transport: t, t_p, t^2, t_p^2 and $t \cdot t_p$.

Incidentally, the appearance of the covariance term in Eq. (19) illustrates the advantage of the correlated sampling approach. If two separate, uncorrelated runs are performed to estimate the perturbed and unperturbed tally responses, the covariance term is zero and the variance of the difference in tally responses is equal to the sum of the variances of the separate runs. Using the correlated sampling approach, the covariance term is large and reduces the error on the estimated difference in response.

4. Specification of transport problems including perturbations

Monte Carlo methods provide a powerful tool for designing and optimising nuclear and X-ray based instruments. An important software design criterion is to build tools that are straightforward for all researchers to use, not just specialists in computer modelling.

Assuming that the user is already familiar with specifying problems for their preferred Monte Carlo package, then the easiest way for them to describe a perturbation problem is to provide separate specifications for the unperturbed and one or more perturbed cases. A pre-processing step then combines these multiple specifications into a single input file that can be executed. The pre-processing step should recognise the different types of perturbations – to materials, geometry and the radiation source – that have been implicitly requested by the user and produce a compact combined problem description that can be run efficiently.

An important consideration for the pre-processor is that it must solve the 'super-set' problem referred to in the previous section. As noted by Rief [7], it is essential that the perturbed weight factor, r_p given by Eq. (2) remains finite so that perturbed particle weights and hence any tally contributions made by these particles are well-defined. The physical interpretation of this requirement is that all process that can occur in the perturbed problem must also occur with non-zero probability in the unperturbed case, otherwise they will not be sampled at all and any tallies in the perturbed problem that depend on these events will be incorrectly estimated.

Examples where this condition cannot be easily satisfied are easy to imagine. For example, a material might contain an element in the perturbed problem that is absent in the unperturbed case. Takahashi's moving reflector block problem (Fig. 1) is another case, where region III is converted from void to solid material in the perturbed problem. A third example might involve changes to the radiation source, such that the energy spectra in the perturbed and unperturbed cases do not completely overlap.

To solve this problem, I use an extension of Rief's 'multiple correlation' technique [7]. Rief proposes the use of a 'reference function' for cases where $p'(\mathbf{x})$ is non-zero but $p(\mathbf{x})$ is zero. Instead of sampling $\mathbf{x}$ from the physical distribution p, one samples from a reference distribution p_0 which is non-zero whenever p or p' is non-zero. Rief proposes two simple forms for p_0, given by either the mean or the maximum of p and p'. I make use of both of these suggested forms.

The way in which I implement the multiple correlation technique is to treat both the unperturbed and perturbed problem variations specified by the user as perturbations of a 'reference case'. The reference case is specifically constructed to ensure that the perturbed weight factor r_p is everywhere finite for both the original, unperturbed problem specified by the user (now handled as the first perturbation of the reference case) and the perturbed problem(s). As such, the reference case is a direct extension of the reference function introduced by Rief.

The first step in constructing the reference case is to build the problem geometry model. The geometry models of the individual problem cases specified by the user each comprise a list of regions, identified by a name which is unique for a given problem case. Each region contains a single material of uniform density and composition.

Two ways of specifying the geometry of individual regions are in common use: surface representation and constructive solid geometry (CSG). A surface representation defines each region in terms of the sense of points within the region with respect to a list of bounding surfaces. The CSG representation describes regions in terms of simple, solid primitives, such as boxes, cylinders, spheres, prisms and volumes of rotation; the basic primitive shape can be augmented by Boolean intersection and difference operations to define more complex shapes. The CSG representation is best suited to solving the problem of creating the reference case geometry model. It is also straightforward to translate from a CSG model to a surface representation for Monte Carlo codes that require this format.

The following algorithm builds the reference case geometry model from the CSG geometry models of the separate problem cases and identifies the material and geometry perturbations required.

1. Create a list of the names of all named regions across all perturbation cases. This list is a concatenation of the lists of names appearing in each perturbation case, with repeats removed.
2. FOREACH region R on the combined list,
   IF R does not appear in all perturbation cases, mark as GEOM
   ELSE
   IF R does not have the same geometry in all cases, mark as GEOM
   ELSEIF R does not contain the same material in all cases, mark as MAT
   ELSE mark as NORMAL
3. FOREACH region R on the combined list marked MAT or NORMAL
   FOREACH region S on the combined list marked GEOM
   IF the definition of S includes the Boolean operation $S - R$, or the definition of R includes the Boolean operation $R \cap S$, mark R as GEOM. The operators $-$ and $\cap$ denote Boolean difference and intersection respectively.
4. Repeat step 3 until no more regions have their designation changed.
5. FOREACH region R on the combined list marked MAT or NORMAL
   FOREACH region S on the combined list marked GEOM
   IF R appears in the Boolean operation $R - S$, mark R as FILLED

This algorithm identifies each region as:

- NORMAL, meaning that no perturbation applies;
- MAT, meaning that a simple material perturbation applies;
- GEOM, meaning that this region is subject to a geometry perturbation; or
- FILLED, meaning that this region, whilst itself unchanged in all perturbation cases, contains in its definition a difference operation involving one or more regions subject to a geometry perturbation.

The reference case geometry model comprises all regions marked NORMAL, MAT or FILLED. Regions marked MAT or FILLED are taken to be filled with a uniform composite material called a 'porridge', which is defined below.

The perturbation geometry models are specified in terms of any differences with respect to the reference case. If a region is defined with the same name as a region appearing in the reference case, the definition in the perturbation model takes precedence. Specifically, the regions that appear in the perturbation definitions are those that appear in the user's original problem specifications and are marked as MAT or GEOM. These regions are filled with the material specified by the user in the original problem definition.

The porridge material used to fill regions in the reference case geometry has a composition and density equal to the arithmetic mean of all the materials appearing in that region across all perturbation cases. For a region marked FILLED, the averaging extends over all regions that lie within the outer boundary of the original primitive volume; these regions can be easily determined by following the chain of Boolean difference operations. For example, if a region R is defined by difference with a second region S, which is in turn defined by difference with a third region T, then the material inside region R in the reference case has the average composition and density of the materials appearing in R, S, and T.

Tracking in regions marked FILLED in the reference case is handled using the modified Woodcock algorithm described in the previous section, with one modification to improve efficiency. When a collision site has been sampled, the reaction occurring at that point is sampled according to the reaction cross-sections of the porridge material *only* if two or more different materials are present at that point in the different perturbed cases. If the regions in all perturbed cases contain the same material at that point, then the appropriate reaction is sampled according to the cross-sections of this material.

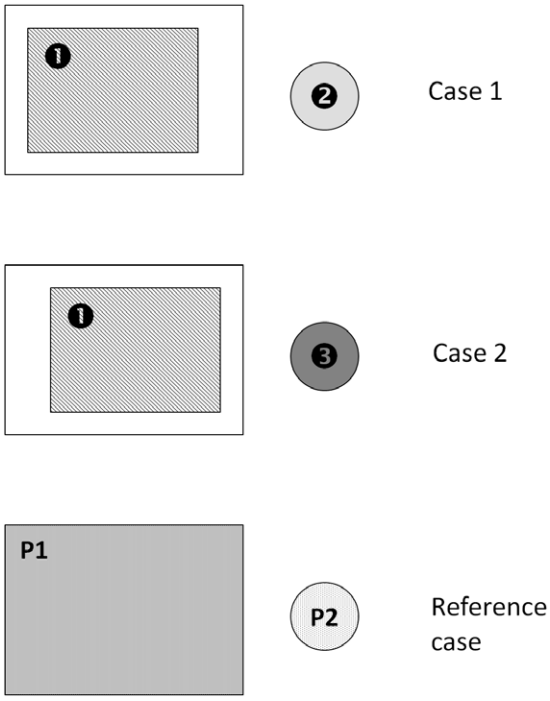

Fig. 2. Construction of reference case geometry model from separate input models specified by user (see text for details).

In regions marked MAT, tracking is handled using the material perturbation algorithm described above. In regions marked NORMAL, regular tracking is used.

Fig. 2 illustrates the algorithm with a simple example. Two geometry cases are defined, both comprising a rectangular region filled with material 1 and a circular region filled with material 2 in case 1, and material 3 in case 2. The rectangular region's position is different in the two cases. In both cases, the rectangular region filled with material 1 is positioned inside a large region (unfilled), which is invariant between the two cases. The definition of this invariant region, which must be specified by the user, serves to limit the size of the volume over which the geometry perturbation tracking algorithm is used. If this region is omitted, then Woodcock tracking will be used over the entire geometry model, with possible adverse performance consequences.

The reference case geometry model contains just two regions: one corresponding to the boundary of the unfilled region that contains the rectangular regions in cases 1 and 2, and the other corresponding to the circular region in the two cases. Both regions are filled with porridge material. The porridge used in the first region arises from averaging vacuum and material one. Consequently, it has the same composition as material one, but one half the density. The porridge used in the second region has a composition given by averaging the elemental concentrations of materials 2 and 3, and a density equal to the arithmetic mean of the densities of these materials. Tracking in the rectangular and circular porridge-filled regions is handled using the geometry and material perturbation algorithms respectively.

The determination of the radiation source specification for the reference case is straightforward. Suppose that the distribution of source radiation quanta with respect to position, $\mathbf{r}$, energy E and polar angle θ (defined with respect to some fixed axis) in the ith

perturbation case is given by $s_i(\mathbf{r}, E, \theta)$; the s_i are normalised to unit area over the available phase–space in position, energy and angle.

The normalised source distribution for the reference case, s, is set equal to

$$s(\mathbf{r}E\theta) = \frac{\max_i s_i(\mathbf{r}, E, \theta)}{\iiint \max_i s_i(\mathbf{r}, E, \theta)\, d\mathbf{r}\, dE\, d\theta} \tag{20}$$

and the starting weight for particles in the ith perturbed case are given simply by s_i/s for the sampled values of $\mathbf{r}$, E and θ.

In many cases of practical interest, the source distribution function is separable. For example, the energy and direction of the source particles are usually independent of the starting position. For an isotropic radioisotope source, the energy and direction of the source particles are also decoupled. If applicable, this separation simplifies the calculation of the source distribution for the reference case.

5. Example application—X-ray fluorescence analyser

To illustrate the application of these techniques, I present results for the simulation of an idealised model of an X-ray fluorescence analysis system. Specifically, the simulation models the irradiation of a copper-bearing material with X-rays emitted by an X-ray tube, and the subsequent detection of copper fluorescence X-rays using a silicon detector.

The perturbation method is used to estimate the effects on the measured fluorescence X-ray intensity of variation in:

1. the operating voltage of the X-ray tube;
2. the position of the X-ray detector;
3. the distance of the sample material from the X-ray tube and X-ray detector; and
4. the composition and density of the sample. In variations 1–3, the sample is assumed to comprise 75% SiO_2, 24% Fe_2O_3 and 1% Cu and has a density of 1.30 g cm^{-3}. In variation 4, the sample comprises 77% SiO_2, 22% Fe_2O_3 and 1% Cu, and has a density of 1.25 g cm^{-3}.

In a real X-ray analyser, variations 1–3 relate directly to the stability of the experimental configuration. Variation 4 illustrates the sensitivity of the analyser to changes in the overall sample composition, with some of the denser, iron-rich matrix of the copper ore replaced with lighter, silicon-rich material.

Fig. 3 illustrates the geometry model and the changes that correspond to variations 2 and 3. The incident X-ray spectrum for tungsten-anode X-ray tube operated at 25 kV with a 0.5 g cm^{-2} aluminium filter to remove low-energy X-rays is calculated using the method described in [16]. Fig. 4 shows this spectrum, along with the perturbed spectrum for variation 1, where the operating voltage is decreased to 24.5 kV.

The Monte Carlo simulation using the perturbation approach then consists of (i) the reference model (ii) the 'base' model and (iii) models corresponding to the four variations. To validate the perturbation approach, separate simulation runs were also performed that directly simulated the base model and four variations. The perturbed model simulation was run for 500 min and the 5 direct simulations for 250 min each on a desktop PC with a 3.00 GHz Intel Core2 Duo processor.

A deposited-energy tally was used to record the spectrum of X-rays interacting in the silicon detector. Fig. 5 compares the simulated spectra for the base model case using direct simulation (solid line) and the perturbation approach (points); the residual differences between the two approaches are plotted below the two spectra. The absence of structure in the residual plot and the root-mean-square residual value of 0.970 (250 degrees

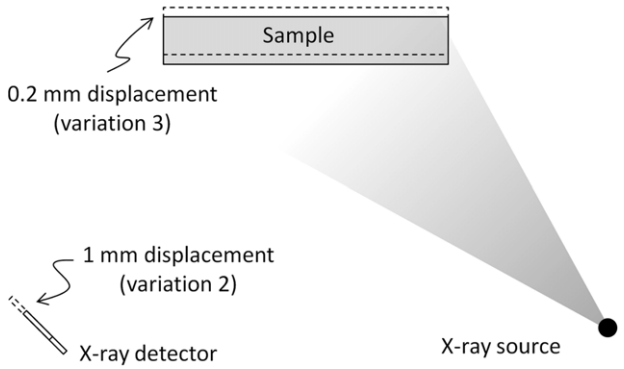

Fig. 3. Model of simple X-ray fluorescence analyser, showing geometric perturbations to sample and detector.

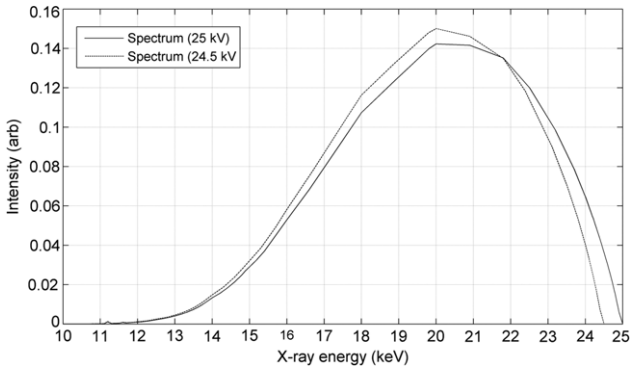

Fig. 4. Simulated X-ray energy spectrum of X-ray tube operated at 25 kV (solid line) and 24.5 kV (dashed line).

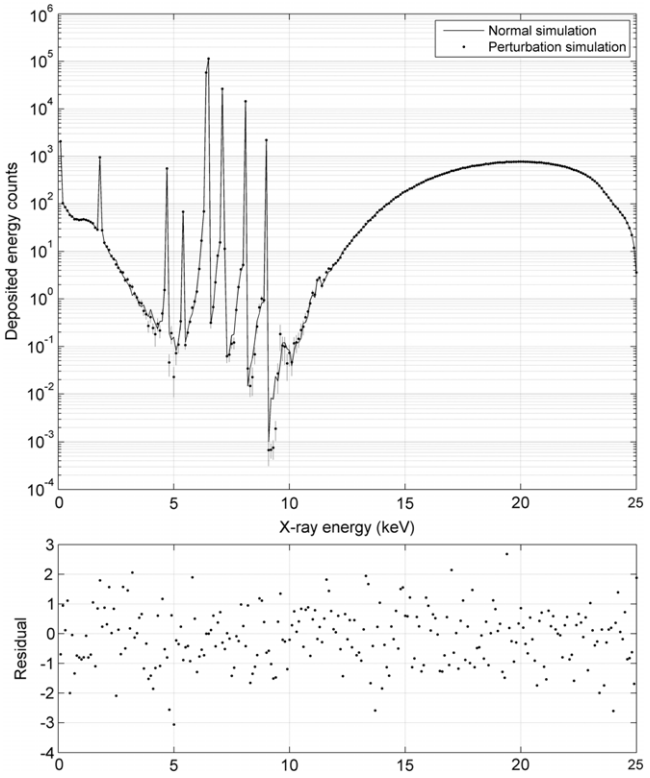

Fig. 5. Comparison of deposited energy X-ray spectrum in the Si-detector calculated using the normal MC method (solid line) and a perturbation approach (points). Residuals between the two methods are shown in the lower figure.

Table 1
Comparison of relative change in copper K-alpha fluorescence intensity for 4 problem variations, estimated using the direct simulation and perturbation methods. Errors in the last digit(s) are shown in brackets.

Variation	Variation ratio, direct method	Variation ratio, perturbation method	Error ratio, direct/perturbation
1	0.9003(19)	0.9022(6)	3.4
2	0.9862(19)	0.9847(9)	2.2
3	0.9862(19)	0.9910(33)	0.6
4	1.0484(20)	1.0492(1)	19

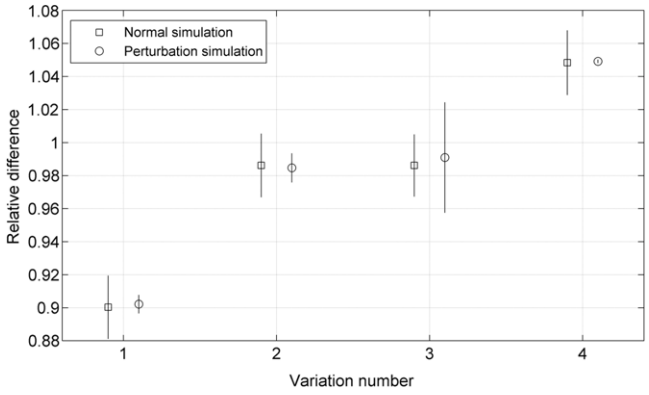

Fig. 6. Comparison of changes in copper fluorescence sensitivity for four variations, calculated from differences between normal simulations (squares) and using the perturbation approach (circles). Error bars show 1-standard deviation statistical errors, multiplied by 10 for visibility. The same total CPU time was used for both approaches.

of freedom) indicate that the two simulations are returning consistent values, which is a powerful check on the correctness of the implementation.

The total number of source events generated in all simulations was very nearly equal, indicating that the perturbation simulation including the reference model, base model case and four variations runs approximately half as fast as the direct simulation. The slowdown reflects the additional computational cost of the perturbation approach. The bin-by-bin statistical errors on the deposition energy spectrum for the two approaches are almost equal.

Table 1 shows the changes in the intensity of the copper K-alpha fluorescence line (the prominent line visible at ∼8 keV in Fig. 5) for the four variations, relative to the base model case. Results are shown for the perturbation approach, and calculated from a simple ratio of the direct simulation results. Statistical errors in the last digit(s) of the intensity ratio are shown in brackets. The same computational effort −500 min—is required for both estimates, remembering that the direct simulation approach requires two separate simulations to be performed.

Fig. 6 plots these results, showing the direct method values as squares and the perturbation method values as circles. Error bars have been multiplied by a factor of 10 to improve visibility.

For three of the four variations, the perturbation method increases the efficiency of the calculation of the change in analyser response. The errors for variations 1, 2 and 4 are 3.4, 2.2 and 19 times smaller respectively, corresponding to a reduction in a CPU time required to achieve a given precision of approximately 12, 5 and 370 times respectively.

For variation 3, the perturbation method is less efficient that the direct simulation method, with an error 1.8 times larger. This variation corresponds to the sample being translated back from the source and detector by 0.2 mm. Although this is a small physical shift, and produces only a small change in the fluorescence intensity, in one important respect this cannot be considered a small perturbation.

The mean-free path of copper fluorescence X-rays is approximately 0.1 mm. Copper X-rays produced in the reference model simulation in the front-most 0.2 mm thick layer that is effectively converted to vacuum in variation 3 may undergo several interactions before escaping from the sample. There is a small but non-vanishing probability of an X-ray undergoing a series of delta interactions, leading to a large perturbed weight for this variation. Close inspection of the simulation output shows that variation 3 does indeed feature a strongly skewed weight distribution compared to the other cases. These high-weight photons increase the variance and reduce the covariance with the reference case, both factors leading to degradation in precision. I anticipate that the weight-windows variance reduction method—that is, selective splitting of high-weight particles to maintain a more consistent weight distribution could be used to help with this problem, but that remains for future testing.

6. Conclusions

I have described an approach for modelling arbitrary perturbations to the geometry model, materials and radiation source used in neutral-particle Monte Carlo simulation. Multiple perturbations can be modelled in a single simulation, providing an efficient means of determining sensitivity to changes in the size, shape, position or composition of components of the model and to variations in the energy spectrum of the radiation source.

Key aspects of the approach include the use of a modified form of the Woodcock algorithm for efficient particle tracking through perturbed volumes and a method for automatically generating the specification of the combined perturbation model from descriptions of the individual perturbations.

The perturbation approach has been applied to a simple model of an X-ray fluorescence analyser, with the sensitivity of the response of the instrument evaluated for changes in X-ray source output, sample composition and the position of the sample and detector. For small perturbations, the method is more computationally efficient than carrying out discrete simulations of the different perturbation cases.

The ability to efficiently calculate difference information for arbitrary changes to a Monte Carlo model is a powerful tool for both instrument design optimisation and for estimating sources of systematic measurement uncertainty in a real analyser.

References

[1] The X-5 Monte Carlo Team, MCNP—a general Monte Carlo N-particle transport code, Version 5, 2005, LA-UR-03-1987.
[2] J.E. Olhoeft, The Doppler Effect for a Non-Uniform Temperature Distribution in Reactor Fuel Elements, WCAP-2048, Westinghouse Electric Corporation, Atomic Power Division, Pittsburgh, 1962.
[3] M.C. Hall, Cross-section adjustment with Monte Carlo sensitivities: application to the Winfrith iron benchmark, Nucl. Sci. Eng. 81 (1982) 423.
[4] B. Morillon, On the use of Monte Carlo perturbation in neutron transport problems, Ann. Nucl. Energy 25 (14) (1998) 1095–1117.
[5] H. Rief, Generalised Monte Carlo perturbation algorithms for correlated sampling and a second order Taylor series approach, Ann. Nucl. Eenrgy 11 (9) (1984) 455–476.
[6] G. Dejonghe, Etudes d'effets différentiels par la méthode de Monte Carlo dans le cadre de l'équation du transport, Applications aux calculs de protection et de neutronique, Ph.D. Thesis, University of Paris XI, Orsay, France, 1982.
[7] H. Rief, A synopsis of Monte Carlo perturbation algorithms, J. Comput. Phys. 111 (1994) 33–48.
[8] H. Rief, Stochastic perturbation analysis applied to neutral particle transport, Adv. Nucl. Sci. Tech. (23) (2002) 69–140.
[9] H. Takahashi, Monte Carlo method for geometrical perturbation and its application to the pulsed fast reactor, Nucl. Sci. Eng. 41 (1970) 259–270.
[10] E. Shuttleworth, The geometrical sensitivity option in MCBEND, in: Proceedings of Monte Carlo 2000, 23–26 October, Lisbon, Portugal, 2000.
[11] S. Sitaraman, Geometric sensitivity analysis using Monte Carlo techniques, Ph.D. Thesis, University of Washington, 1984.

[12] I. Kawrakov, E. Mainegra-Hing, D.W.O. Rogers, F. Tessier, B.R.B. Walters, The EGSnrc Code System: Monte Carlo Simulation of Electron and Photon Transport NRCC Report PIRS-701, 2011. Available online at http://www.irs.inms.nrc.ca/EGSnrc/pirs701.pdf (accessed 04.08.11).
[13] E.R. Woodcock, et al., Techniques used in the GEM code for Monte Carlo neutronics calculations in reactors and other systems, in: Proc. Conf. Applications of Computing Methods to Reactor Problems, ANL-7050, 1965.
[14] D. Tucker, G. Barnes, D. Chakraborty, Semiempirical model for generating Tungsten target X-ray spectra, Med. Phys. 18 (2) (1991) 211–218.
[15] D. Tucker, G. Barnes, W. Xizeng, Molybdenum target X-ray spectra: a semiemperical model, Med. Phys. 18 (3) (1991) 402–407.
[16] H. Ebel, X-ray tube spectra, X-ray Spectra (28) (1999) 255–266.
[17] M.H. Kalos, Nucl. Sci. Eng. (16) (1963) 111.
[18] E. Williams, J. Tickner, Efficient Monte Carlo simulation of coincidence effects in radioisotope decays including $\gamma - \gamma$ angular correlations, Comput. Phys. Comm. 183 (9) (2012) 1869–1876.
[19] T.E. Booth, Monte Carlo Variance Reduction Approaches for Non-Boltzmann Tallies, Los Alamos Report LA-12433, 1992.